Remote Sensing of Environment 121 (2012) 144–158

Contents lists available at SciVerse ScienceDirect

Remote Sensing of Environment

journal homepage: www.elsevier.com/locate/rse

Greenness in semi-arid areas across the globe 1981–2007 — an Earth Observing Satellite based analysis of trends and drivers

Rasmus Fensholt [a,*], Tobias Langanke [a], Kjeld Rasmussen [a], Anette Reenberg [a], Stephen D. Prince [b], Compton Tucker [c], Robert J. Scholes [d], Quang Bao Le [e,f], Alberte Bondeau [g,o], Ron Eastman [h], Howard Epstein [i], Andrea E. Gaughan [j], Ulf Hellden [n], Cheikh Mbow [k], Lennart Olsson [n], Jose Paruelo [l], Christian Schweitzer [m], Jonathan Seaquist [n], Konrad Wessels [d]

[a] Department of Geography and Geology, University of Copenhagen, Oster Voldgade 10, 1350 Copenhagen, Denmark
[b] Department of Geography, 2181 LeFrak Hall, University of Maryland, College Park MD 20742, USA
[c] NASA Goddart Space Flight Center, Mail Code 514, Greenbelt, MD 20771, USA
[d] Council for Scientific and Industrial Research (CSIR), PO Box 395, Pretoria 0001, South Africa
[e] University of Bonn, Center for Development Research (ZEF), Walter-Flex-Str. 3, D-53113 Bonn, Germany
[f] Institut f. Umweltentscheidungen, ETH Zürich, Universitätstrasse 16, 8092 Zürich, Switzerland
[g] Potsdam Institute for Climate Impact Research, Telegrafenberg, P.O. Box 60 12 03, D-144 12 Potsdam, Germany
[h] Clark University, Graduate School of Geography, 950 Main Street, Worcester, MA 01610, USA
[i] Department of Environmental Sciences, University of Virginia, Clark Hall, 291 McCormick Road, P.O. Box 400123, Charlottesville, VA 22904-4123, USA
[j] University of Florida, Department of Geography, 3141 Turlington Hall, PO Box 117315, Gainesville, FL 32611-7315, USA
[k] Institut des Sciences de l'Environnement, Université Cheikh Anta Diop de Dakar, Senegal
[l] Facultad de Agronomía/IFEVA, Universidad de Buenos Aires and CONICET, Av. San Martín 4453, 1417 Buenos Aires, Argentina
[m] Helmholtz Centre for Environmental Research — UFZ, Department Computational Landscape Ecology – CLE, Permoser Str. 15, D-04318 Leipzig, Germany
[n] Department of Earth and Ecosystem Sciences, Lund University, Sölvegatan 12, 223 62 Lund, Sweden
[o] Institut Méditerranéen de Biodiversité et d'Ecologie marine et continentale (IMBE) (Mediterranean Institute for Biodiversity & Ecology)UMR CNRS 7263 / IRD 237, Bâtiment Villemin, Europole de l'Arbois - BP 80F-13545 Aix-en-Provence cedex 04, France

ARTICLE INFO

Article history:
Received 13 July 2011
Received in revised form 17 January 2012
Accepted 21 January 2012
Available online xxxx

Keywords:
AVHRR GIMMS NDVI
MODIS NDVI
Semi-arid
Vegetation greenness
Phenology
Precipitation
Air temperature
Incoming shortwave radiation

ABSTRACT

Semi-arid areas, defined as those areas of the world where water is an important limitation for plant growth, have become the subject of increased interest due to the impacts of current global changes and sustainability of human lifestyles. While many ground-based reports of declining vegetation productivity have been published over the last decades, a number of recent publications have shown a nuanced and, for some regions, positive picture. With this background, the paper provides an analysis of trends in vegetation greenness of semi-arid areas using AVHRR GIMMS from 1981 to 2007. The vegetation index dataset is used as a proxy for vegetation productivity and trends are analyzed for characterization of changes in semi-arid vegetation greenness. Calculated vegetation trends are analyzed with gridded data on potential climatic constraints to plant growth to explore possible causes of the observed changes. An analysis of changes in the seasonal variation of vegetation greenness and climatic drivers is conducted for selected regions to further understand the causes of observed inter-annual vegetation changes in semi-arid areas across the globe. It is concluded that semi-arid areas, across the globe, on average experience an increase in greenness (0.015 NDVI units over the period of analysis). Further it is observed that increases in greenness are found both in semi-arid areas where precipitation is the dominating limiting factor for plant production (0.019 NDVI units) and in semi-arid areas where air temperature is the primarily growth constraint (0.013 NDVI units). Finally, in the analysis of changes in the intra-annual variation of greenness it is found that seemingly similar increases in greenness over the study period may have widely different explanations. This implies that current generalizations, claiming that land degradation is ongoing in semi-arid areas worldwide, are not supported by the satellite based analysis of vegetation greenness.

1. Introduction

Drylands are intrinsically characterized by scarcity of water but many different definitions exist. The World Atlas of Desertification (United Nations Environment Programme et al. (1997)) defines

* Corresponding author. Tel.: +45 353 22526; fax: +45 35322501.
E-mail address: rf@geo.ku.dk (R. Fensholt).

0034-4257/$ – see front matter © 2012 Elsevier Inc. All rights reserved.
doi:10.1016/j.rse.2012.01.017

drylands as those areas with an aridity index (AI, the ratio between mean annual precipitation and mean annual potential evaporation) below 0.65. The areas investigated in this paper are confined to those with an AI between 0.2 and 0.5 (semi-arid), based on the World Atlas of Desertification (Fig. 1A) due to the well known uncertainty of NDVI estimates for sparse vegetation (Huete et al., 1985) that can cause spurious trends depending on the sensor (Fensholt & Proud, 2012).

The semi-arid areas constitute around 15% of the global land area and are estimated to be the home of approximately 15% of the global human population (Millennium Ecosystem Asessment, 2005). Semi-arid ecosystems provide food, grazing for livestock, energy, forestry products and ecosystems services, and the sustainability of these is a concern. Especially since the Sahel drought of the 1970s and 80s and high level UN Conferences in 1977 and 1992 there has been widespread interest in environmental trends and problems of poverty and economic development in semi-arid areas, particularly in developing countries. The official UNCCD definition of desertification, equating it with land degradation in drylands, implies that change in vegetation productivity is a key metric (but not the only one) of land degradation. Furthermore, vegetation productivity is of great economic significance because crop and livestock production in many semi-arid regions is the primary economic activity and a key supporting ecosystem service, as defined by the Millennium Ecosystem Asessment (2005). Therefore, spatially and temporally consistent, long-term data on changes and trends in vegetation productivity are of great interest for the assessment of environmental conditions in dryland regions. Only Earth Observation (EO) satellite data provide suitable, global, temporally and spatially consistent data, with a medium-term time-series covering the last 3 decades.

While many reports of declining vegetation productivity in arid and semi-arid lands using ground based measurements have been published over the last decades, a recent and authoritative example being the Millennium Ecosystem Asessment (2005), recent publications based on the use of EO-data have shown a more nuanced picture with both declines and increases (Bai et al., 2008; Beck et al., 2011), with several papers focusing on the 'greening of the Sahel' (see e.g. Anyamba and Tucker, 2005; Hellden and Tottrup, 2008; Hickler et al., 2005 and Prince et al., 2007). These publications have been based on a variety of different EO datasets and they use slightly different methods.

Our paper provides a global analysis of the trends in vegetation greenness in Earth's arid and semi-arid lands, as assessed from the Advanced Very High Resolution Radiometer (AVHRR) sensor on board the US NOAA (National Oceanic and Atmospheric Administration) series of satellites from 1981 to 2007. The 'Normalized Difference Vegetation Index' (NDVI), computed from the AVHRR data, is used as a proxy for vegetation productivity. Trends in NDVI may be related to climatic as well as non-climatic causes of change (e.g. management), and it is obviously of great policy relevance to better attribute the drivers of observed NDVI trends.

The main questions this paper addresses are:

1) What is the quality of the GIMMS NDVI data for the semi-arid areas across the globe?
2) What are the trends of vegetation greenness in semi-arid areas across the globe over the period 1981–2007?
3) What can be said, at global and regional scales, about the causes of the observed trends in vegetation greenness by studying trends in potential climatic constraints to vegetation growth (precipitation, air temperature and incoming shortwave radiation)?
4) Does analysis of changes in intra-annual NDVI trends in conjunction with information on intra-annual trends of climatic constraints to vegetation growth add to the understanding of causes for observed NDVI trends?

Land cover classes of semi-arid areas across the globe are shown for year 2000 in Fig. 1B (Global land cover from SPOT VGT, Bartholomé et al., 2002) and climatic plant growth constraints based on long-term monthly climate statistics, as developed by Nemani et al. (2003) are shown in Fig. 1C. These maps function as a reference for further analysis and discussions of observed vegetation trends in semi-arid areas.

2. Data

2.1. NDVI products

The widely-used AVHRR GIMMS-g NDVI archive (Tucker et al., 2005) was selected for the current analyses. At present the GIMMS-g data archive is the only global coverage dataset spanning 1981 to recent time that is subjected to ongoing validation. The GIMMS-g archive is considered the best dataset available for long-term NDVI trend analysis (Beck et al., 2011). The original 8 km spatial resolution GIMMS 15-day NDVI composite data covering the period from July 1981 to December 2007 were aggregated to months using a maximum value composite approach to further reduce the influence from clouds and to match the temporal resolution of the MODIS product used for comparison.

The more recent high quality MODIS (Moderate Resolution Imaging Spectroradiometer) data (Huete et al., 2002), covering the Feb. 2000 — present time was used to study the quality of the GIMMS NDVI data record. The MODIS data used are the NDVI 0.05 degree monthly product (MOD13C2, collection 5) which is based on spatial and temporal averages of 16-day 1-kilometer NDVI (MOD13A2) (Solano et al., 2010). MOD13A2 is processed from MODIS level 2 (L2G) daily surface reflectance product (MOD09 series), providing red and near infrared surface reflectance corrected for the effects of atmospheric gasses, thin cirrus clouds and aerosols. The MOD09 band 1–7 product is an estimate of the surface spectral reflectance as would be measured at ground level if there were no atmospheric scattering or absorption (Vermote et al., 2002). MODIS red and near-infrared reflectance data (included in MOD13C2, collection 5) have been resampled to match the GIMMS resolution by spatial averaging before calculating NDVI used for the direct comparison.

2.2. Climatic drivers

The precipitation data used is the blended gage-satellite GPCP 2.1 product (Adler et al., 2003) provided in a 2.5 degree spatial resolution covering the full period of AVHRR data. Air temperature data are the NOAA NCEP CPC GHCN_CAMS (National Oceanic and Atmospheric Administration, National Centers for Environmental Prediction, Climate Prediction Center, Global Historical Climatology Network, Climate Anomaly Monitoring System) 0.5 degree gridded global monthly land surface air temperature (Fan and van den Dool, 2008). Incoming shortwave radiation is based on NOAA NCEP-DOE (Department of Energy) Reanalysis-2 gridded global monthly incoming shortwave radiation data (Kanamitsu et al., 2002) provided in a 1.875 degree grid.

Precipitation, air temperature and incoming shortwave radiation data are resampled to preserve the 8 km spatial resolution of the NDVI data (as in Herrmann et al., 2005) using a nearest neighbor algorithm replicating the pixels without changing the original cell values.

Fig. 1. (A) Humidity classes as defined in "The world atlas of desertification" (UNEP, 1997). (B) Global land cover (GLC-2000) for the semi-arid areas. (C) Geographic distribution of potential climatic constraints to plant growth (Nemani et al., 2003) for the semi-arid areas overlaid by areas (white circles and lines) selected for analysis of seasonality (used in Fig. 9).

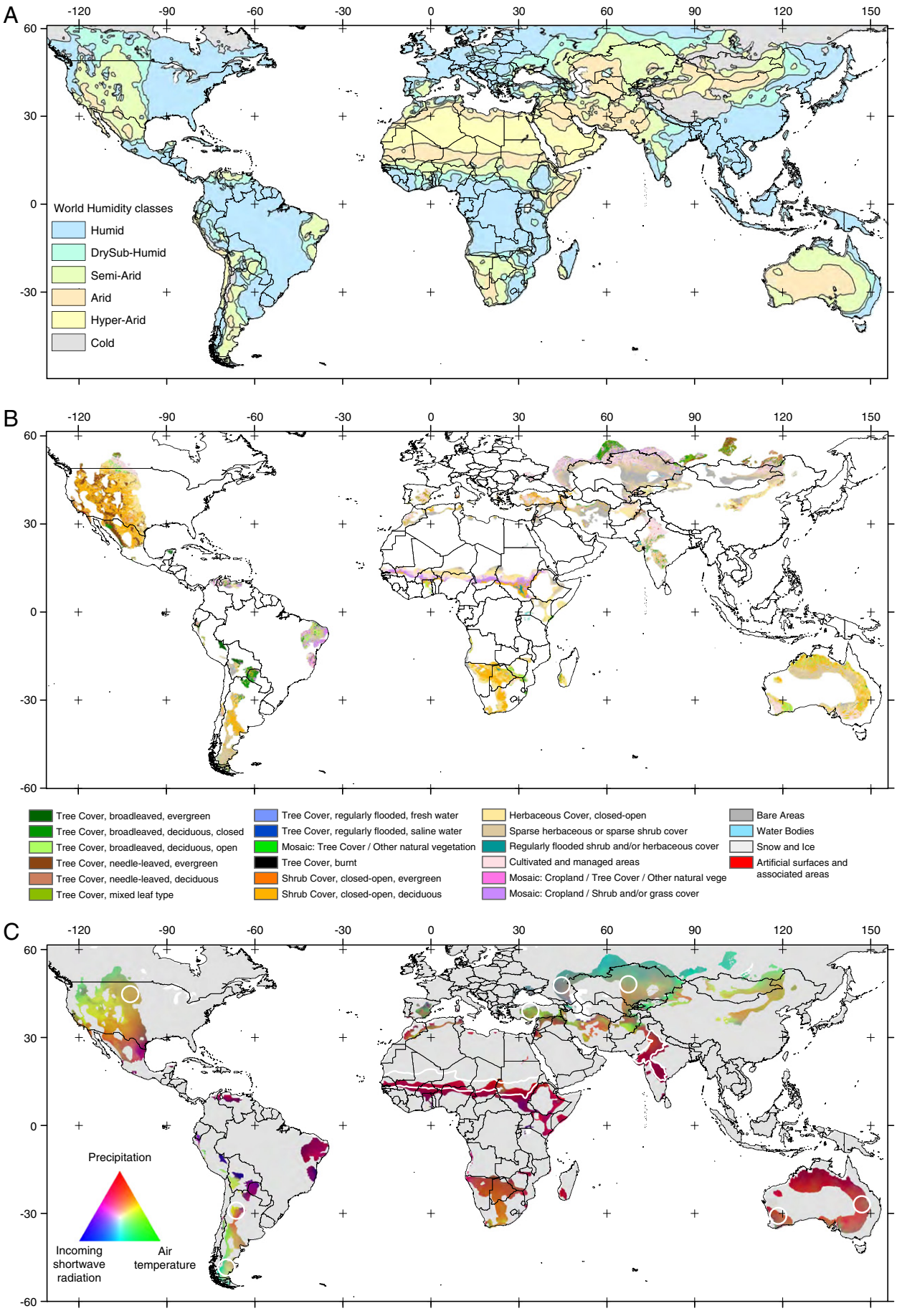
A
B
C
-120
-90
-60
-30
0
30
60
90
120
150
60
30
0
-30
-60
World Humidity classes
Humid
DrySub-Humid
Semi-Arid
Arid
Hyper-Arid
Cold
Tree Cover, broadleaved, evergreen
Tree Cover, broadleaved, deciduous, closed
Tree Cover, broadleaved, deciduous, open
Tree Cover, needle-leaved, evergreen
Tree Cover, needle-leaved, deciduous
Tree Cover, mixed leaf type
Tree Cover, regularly flooded, fresh water
Tree Cover, regularly flooded, saline water
Mosaic: Tree Cover / Other natural vegetation
Tree Cover, burnt
Shrub Cover, closed-open, evergreen
Shrub Cover, closed-open, deciduous
Herbaceous Cover, closed-open
Sparse herbaceous or sparse shrub cover
Regularly flooded shrub and/or herbaceous cover
Cultivated and managed areas
Mosaic: Cropland / Tree Cover / Other natural vege
Mosaic: Cropland / Shrub and/or grass cover
Bare Areas
Water Bodies
Snow and Ice
Artificial surfaces and associated areas
Precipitation
Incoming shortwave radiation
Air temperature

3. Methods

The 27-year series of AVHRR GIMMS NDVI was investigated for semi-arid areas across the globe to analyse changes in inter- and intra-annual trends as a function of the primary potential climatic constraints to infer possible causes for observed inter-annual changes in greenness. Four methods were used to answer the questions raised in the introduction: (1) GIMMS data was compared to MODIS NDVI using linear correlation analysis; (2) long-term trend analyses of NDVI were conducted; (3) trend analysis of climatic variables and correlation analysis between NDVI and climate variables was conducted; and (4) analysis of trends in intra-annual NDVI (changes in phenology) was calculated and compared to analyses of intra-annual trends of primary climatic constraints to vegetation growth.

3.1. Linear correlation analysis

The quality of GIMMS NDVI data is assessed from the strength of linear association between GIMMS and MODIS datasets by calculating the per-pixel Pearson product moment correlation coefficient (r) from 8-years of overlapping monthly observations (Feb. 2000 to Dec. 2007, n = 95). The linear association between GIMMS NDVI and potential climatic constraints to vegetation growth is determined using single (r-value) and multiple regression (adjusted r^2 value) analyses. An annual time-step (starting in Jan. 1982) is used to minimize lag effects between climatic driver and vegetation growth. The relations between annually summed GIMMS NDVI and annually summed precipitation, annually averaged air temperature and annually summed estimates of incoming shortwave radiation are assessed for the 26 years series of data.

3.2. Trend estimation

Long term changes in vegetation greenness do not necessarily develop uniformly through the series as has been reported in many region-global scale analyses (Donohue et al., 2009; Hellden and Tottrup, 2008; Herrmann et al., 2005; Nemani et al., 2003; Olsson et al., 2005). The long-term trend analyses performed here, therefore, used different approaches (1) the Mann−Kendall (MK) monotonic test on trends (providing the possibility of testing for non-linear development in NDVI) and (2) Pearson Product–moment linear correlation test on trends (here referred to as the linear model (LM) providing the possibility of testing for linear development in NDVI). The Theil–Sen median slope trend analysis, which is a linear trend calculation that is resistant to the impact of outliers (noise) was used to quantify the NDVI trend (magnitude of change over time). All tests were performed on GIMMS 8 km data on a per-pixel basis.

The MK test measures the degree to which a trend is consistently increasing or decreasing (range from −1 to +1) (Kendall, 1938) and is recently used for global coverage vegetation analysis in de Jong et al. (2011). A value of +1 indicates a trend that continuously increases and a value of −1 if it always decreases. A value of 0 indicates no consistent trend. The calculation is based on pair-wise combinations of values over time and the statistic is simply the relative frequency of increases minus the relative frequency of decreases. Observations characterized by a strong change over time but with values fluctuating moderately from year-to-year will produce a value close to 0 with this technique. The Pearson Product–moment linear correlation (r values having a range from −1 to 1) is used for testing trends by estimating the linear correlation between the values of each pixel over time and a perfectly linear series.

The tests (MK and the LM) on NDVI trends were compared by calculating a difference map. Both test outputs have a range from −1 to 1 and a comparison will allow for studying the NDVI trends further in respect to linearity/non-linearity despite differences in the calculation of MK and the LM values. The spatial distribution of a difference map will reveal any regions where a LM test does not describe NDVI trends equally well as MK test. When comparing the two tests, pixels characterized by positive MK values and LM output values were analyzed separately from pixels characterized by negative values in both tests to facilitate the interpretation of the analyses output (if not separated the information on the overall direction of the per-pixel NDVI trend (positive/negative) will be lost).

The Theil–Sen median slope is a robust trend statistical method (Hoaglin et al. (2000); Sen, 1968; Theil, 1950) calculating the median of the slopes between all n(n-1)/2 pair wise combinations over time. This method is related to linear least square regression trend techniques (Fensholt et al., 2009; Hellden and Tottrup, 2008; Herrmann et al., 2005; Olsson et al., 2005), however, it is based on non-parametric statistics and is particularly effective for the estimation of trend in small and noisy series. Because it is based on the median, approximately 29% of the samples can be unrelated noise and have no impact on the statistic (Hoaglin et al., 2000). The value of the slope of the line fitted to the NDVI-time data indicates the rate at which the change in greenness has taken place. Slope values represent the total increase/decrease in NDVI over the 318 months between July 1981 and December 2007 measured on a NDVI scale from −1 to +1.

The NDVI time-series was corrected for serial correlation (auto-correlation) using a prewhitening approach before testing the significance of the observed trends. Prewhitening refers to the removal of serial correlation in the residuals of NDVI while preserving the trend. The trend preserving prewhitening uses the procedure described by Wang and Swail (2001) where an iterative procedure is used to separate the true serial correlation and the trend-preserving prewhitened series. The prewhitened series has the same trend as the original series, but with no serial correlation (Wang and Swail, 2001). After prewhitening the significance was tested using a MK significance test producing z scores which provide information on the significance of the trend (Fig. 3).

3.3. Assigning potential climatic drivers to NDVI trends

The output of the long-term trend analysis performed on NDVI (Section 4.2) was analyzed as functions of climatic plant growth constraints, as developed by Nemani et al. (2003). The relative importance of climatic controls (precipitation, incoming shortwave radiation and air temperature) for vegetation growth was assigned to each pixel. In cases where one variable has a predominant control on plant growth (i.e. one variable exceeded the sum of the other two), the pixel slope value was extracted for further statistical analysis.

3.4. Intra-annual trend analysis

Changes in seasonality and phenology were explored with Seasonal Trend Analysis (STA, Eastman et al., 2009) that has two stages; (1) harmonic regression; and (2) a non-parametric linear trend procedure. Harmonic regression was applied per-pixel over the 26 years of monthly images to extract the mean annual image, the annual cycle and the semi-annual cycle (described by 5 harmonic shape parameters). This technique is similar in character to Fourier analysis as used by Hill et al. (2008). The use of two harmonics provides a generalization of the seasonal curve that balances the need to describe the basic structure of the time series while avoiding excessive influence of noise (Eastman et al., 2009). The per-pixel trends in the harmonic shape parameter images were analyzed using the Theil–Sen median slope operator by calculating the slope for each pair wise combination of samples through time (26 years). The calculated trends of median slope and intercept values on each of the five shape parameters for the 26 years were then translated into seasonal curves for a specified number of years to represent the seasonality for the beginning and end of the series (Eastman et al., 2009). Two groups of six years were used (1982–1987 and 2002–2007) in the

Table 1
Details of sample areas selected for analysis of seasonality based on NDVI slope values and potential climatic constraints.

	Constrained by water availability				Equally constrained by water and air temperature			
	Area	Pixel counts	Km^2	Center coordinate	Area	Pixel counts	Km^2	Center coordinate
Positive NDVI trends dominating	Sahel (Shape)	47,421	3,034,944	Not applicable	Turkey (Circle)	2000	128,000	39.1°N 33.4°E
	India (Shape)	18,570	1,188,480	Not applicable	N. & S. Dakota (Circle)	2000	128,000	46.5°N 101.5°W
	W. Australia (Circle)	2000	128,000	30.5°S 118°E	SW. Russia (Circle)	2000	128,000	47.0°N 66.4°E
Negative NDVI trends dominating	N. Argentina (Circle)	2000	128,000	29.0°S 66.4°W	S. Argentina (Circle)	2000	128,000	48.0°S 69.0°W
	E. Australia (Circle)	2000	128,000	26.3°S 147.0°E	C. Kazakhstan (Circle)	2000	128,000	46.4°N 45.4°E

transformation to reduce the influence of single-year anomalies on the output seasonal curves.

Ten areas representing combinations of significant positive and negative trends and climatic constraints to plant growth were selected to study intra-annual changes (seasonality or phenology) in order to explore potential causes of the trends observed (Table 1 and Fig. 1C). The areas selected were contiguous samples of pixels defined by the direction of the NDVI trend and the categories of limiting factors. As expected, no large semi-arid areas of significant NDVI trends characterized by being primarily constrained by either incoming

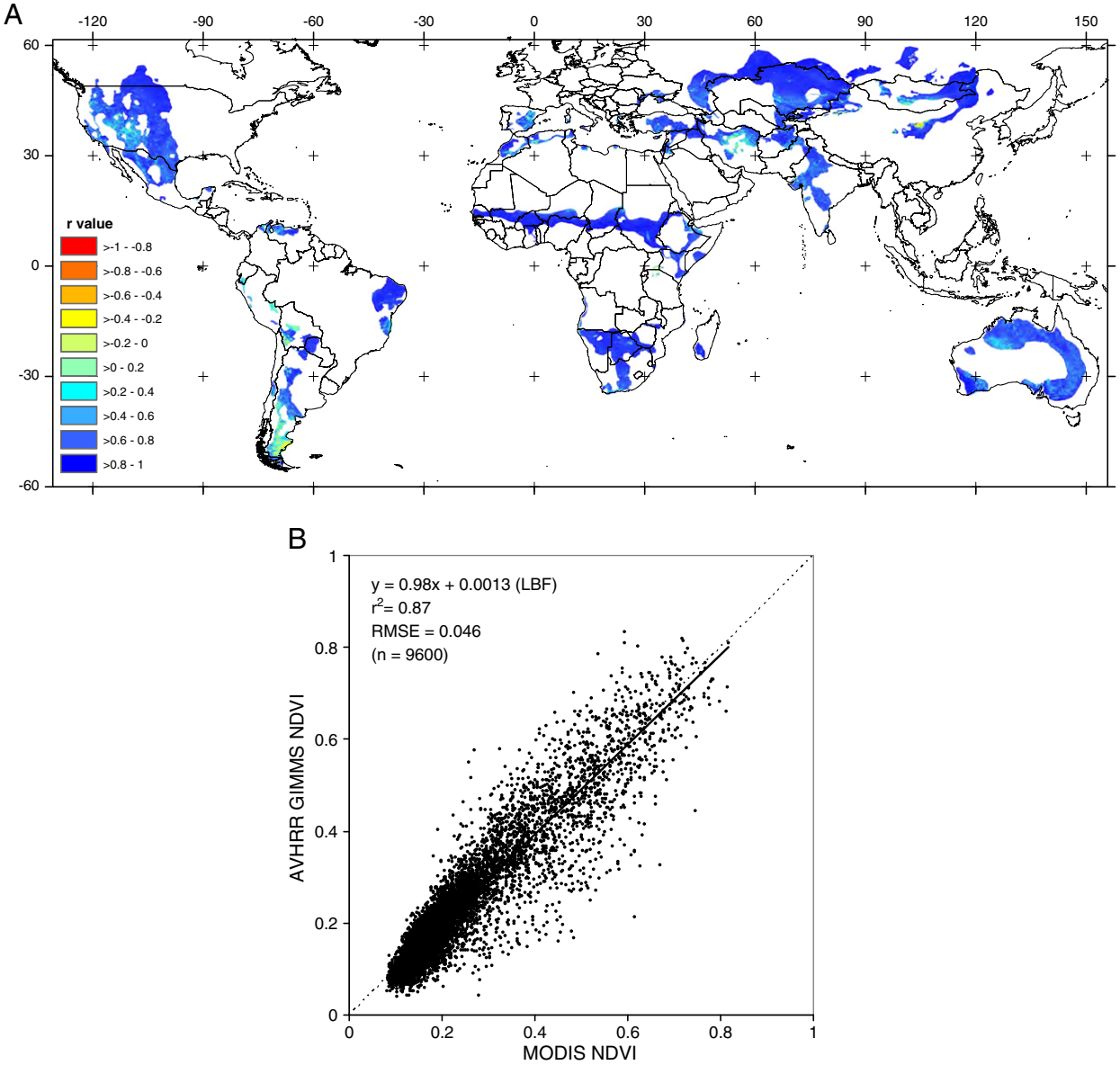

Fig. 2. (A) Map of r-values for monthly NDVI GIMMS correlated against monthly NDVI MODIS Feb. 2000–Dec. 2007. (B) Scatterplot of monthly NDVI MODIS against monthly NDVI GIMMS Feb. 2000–Dec. 2007 for 100 pixels randomly selected in the Sahel. Dashed line represents the 1:1 line and black line is the line of best fit (LBF).

shortwave radiation or air temperature were found; hence these categories were omitted from the intra-annual change analysis. A category was added to include pixels equally influenced by precipitation and air temperature constraints.

4. Results

4.1. GIMMS NDVI quality assessment

A high correlation between the GIMMS NDVI dataset and the well-calibrated and atmospherically corrected MODIS dataset for the overlapping period 2000–2007 can be observed for most semi-arid areas across the globe (Fig. 2A). Areas of low absolute r-values are associated with low year-round NDVI values bordering the arid zone (e.g. in southern Argentina, western US and central Iran) thereby causing a low dynamic range in the NDVI data for the linear correlation analysis. A scatterplot of monthly observations of MODIS and GIMMS NDVI for 100 pixels selected randomly within Sahel (Fig. 2B) shows high correlation ($r^2 = 0.87$) and a line of best fit (LBF) close to a 1:1 line indicating good correspondence between the two NDVI products.

4.2. Inter-annual trends in observed NDVI

The changes in NDVI (Fig. 3a) show that, while there are regions of increased and decreased NDVI, there was a noticeable trend of greening of the semi-arid zone across the globe (288,123 of 438,481 pixels with a positive trend (66%)). Using the significance test described above, 36% and 27% of the semi-arid pixels were characterized by significant change values (both positive and negative) at the 0.05 and 0.01 significance levels respectively and out of the pixels with a significant positive/negative trend 77% and 78% was characterized by positive trends at the 0.05 and 0.01 significance levels respectively. The changes in NDVI across the globe varied between regions, and there were areas with considerably higher rates of change as expressed by the standard deviation of the slope values (0.035 (NDVI units over the full period of analysis), Table 2). The average slope value (Table 2) was 0.015 (NDVI units over the full period of analysis), indicating an overall greening for semi-arid areas across the globe over the 27 years.

Both MK and LM tests were applied to study the consequence of assuming a linear trend development in the 27 years NDVI series. For areas of positive NDVI trend values in Fig. 3, it is clear that the greater part of the global semi-arid changes is described better using a LM as compared to MK (Fig. 4A) (mean difference value of 0.039; Table 2). However, there were areas in central Australia and the temperate zones of China, Mongolia, and Russia where MK test values attained higher values as compared to the LM test. Conversely, for areas with negative NDVI changes, when subtracting the LM and MK test output values (Fig. 4B), the general pattern was that the MK test better described the NDVI trends as compared to the LM test (mean difference value of −0.019; Table 2).

4.3. Inter-annual NDVI trend relationship with climatic drivers

In semi-arid areas vegetation growth is usually limited by precipitation, yet other factors, such as air temperature, incoming shortwave radiation and nutrients may also be involved. Using maps of the relative importance of precipitation, air temperature and incoming shortwave radiation for vegetation across the globe by Nemani et al. (2003) (Fig. 1C), the semi-arid areas analyzed in this paper were categorized according to the dominant limiting factors (precipitation, air temperature and incoming shortwave radiation) and NDVI trends were analyzed for each category. Semi-arid areas mainly constrained (as defined here (Section 3.3)) by precipitation occupied 50.5% (221,324 pixels), 7.3% mainly by air temperature (31,830 pixels) and 0.2% mainly by incoming shortwave radiation (683 pixels). The remaining 42.1% of semi-arid pixels are not characterized by a single predominant driver as being defined in Section 3.3. The NDVI slope values of these three categories of potential climatic constraints to plant growth are shown as histograms in Fig. 5A–C. NDVI trends for semi-arid areas across the globe were found to be positive on average irrespective of whether precipitation (mean NDVI slope of 0.019), air temperature (mean NDVI slope of 0.013) or incoming shortwave radiation (mean NDVI slope of 0.015) was considered to be the main limiting factor for growth.

The slope values of the NDVI trends plotted against the standardized z scores for the different climatic constraints are shown in Fig. 6. The majority of pixels are characterized by positive trends (1 quadrant) for both precipitation and air temperature constrained environments. The bulk of pixels characterized by negative trends (3 quadrant) was found to be mostly associated with semi-arid areas of South America (Fig. 3) constrained by a blend of precipitation and air temperature (Fig. 1C), while more dispersed patterns of negative trends are found in southern Africa, southern USA bordering Mexico, Australia, Jordan, Iraq and Afghanistan are all primarily limited by precipitation. In semi-arid areas of Kazakhstan, Inner Mongolia and

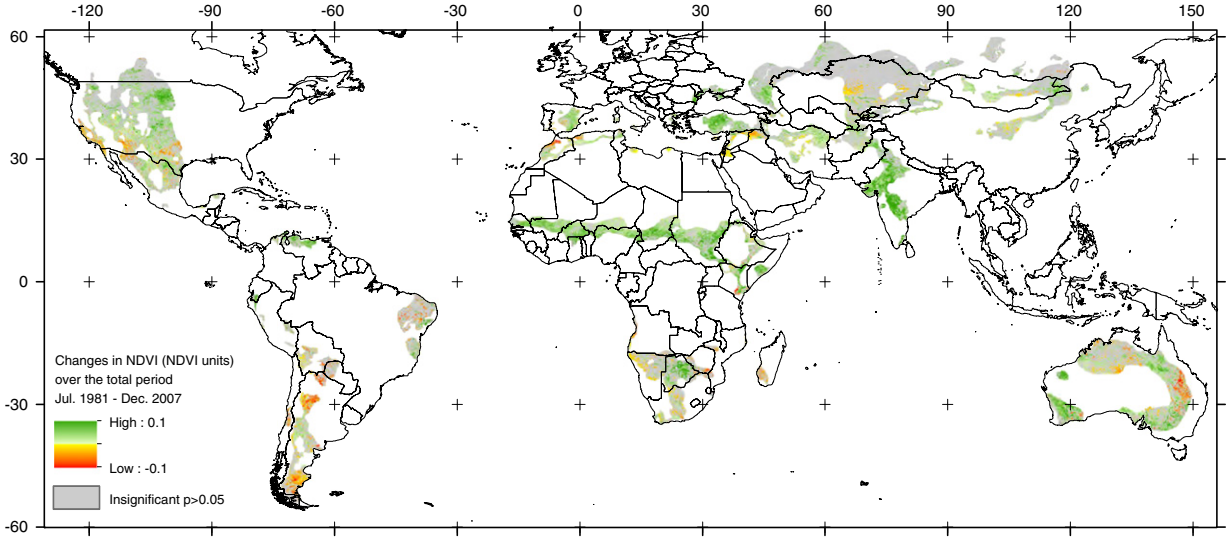

Fig. 3. Changes in NDVI for semi-arid areas from July 1981 to December 2007. Only pixels with a statistically significant trend ($p<0.05$) are colored. (For interpretation of the references to color in this figure legend, the reader is referred to the web version of this article.)

Table 2
Statistics of per-pixel average NDVI trends (1981–2007) in semi-arid areas for linear and non-linear trends. Statistics are provided as NDVI units over the full period of analysis.

Metric/analysis	Count	Minimum	Maximum	Mean	Std dev.
NDVI median slope (linear trend)	438,481	−0.181	0.329	0.015	0.035
Difference between linear and non-linear trends for areas of positive trends (both metrics)	278,592	−0.169	0.285	0.039	0.037
Difference between linear and non-linear trends for areas of negative trends (both metrics)	126,290	−0.246	0.158	−0.019	0.029

north-central China negative trends are found (Fig. 3) for areas constrained both by precipitation and air temperature (Fig. 1C).

Significant slope values ($p<0.05$) of precipitation and air temperature 1982–2007 based on linear trend analyses are shown in Fig. 7A–B (incoming shortwave radiation is omitted from this analysis due to the limited number of pixels belonging to the semi-arid class constrained primarily by incoming shortwave radiation).

Annual integrals of NDVI for semi-arid areas (1982–2007) are correlated with annual values of precipitation and air temperature (Fig. 8A and B) to study the spatial distribution of the strength of these relationships and their correspondence with the spatial distribution of the variable being the a priori primary climatic constraint to growth (Fig. 1C). Summaries of the NDVI trends for each climatic constraint variable (Table 3) show that 52% of pixels within semi-arid areas constrained predominantly by precipitation are characterized by significant NDVI trends ($p<0.05$). 32% of the pixels in air temperature constrained semi-arid areas were found to be significant. Pixels of significant NDVI trends within each (major) constrained semi-arid area, also with a corresponding positive/negative significant trend in the driver variable (precipitation and air temperature) are given in Table 3. Results show that 45% of significant NDVI trends in water constrained areas also have a significant trend in precipitation whereas 75% of significant NDVI trends in air temperature constrained areas also show significant trends in air temperature. The degree of

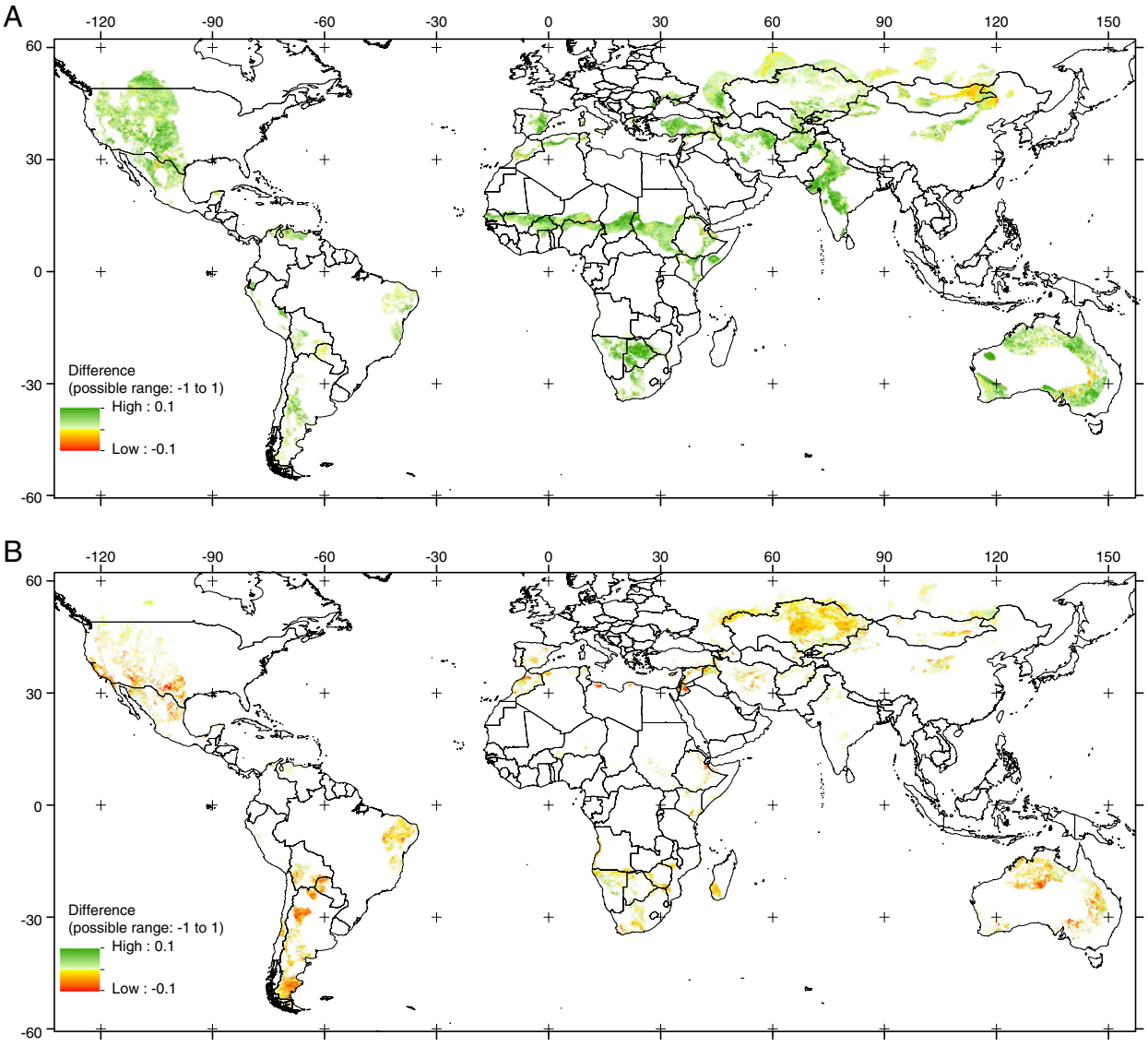

Fig. 4. Per-pixel difference between LM test and Mann–Kendall test on NDVI trends in semi-arid areas (July 1981 to December 2007) (A) for areas of positive NDVI trends (Fig. 3) (B) for areas of negative NDVI trends (Fig. 3). In both cases MK test values were subtracted from the LM test values.

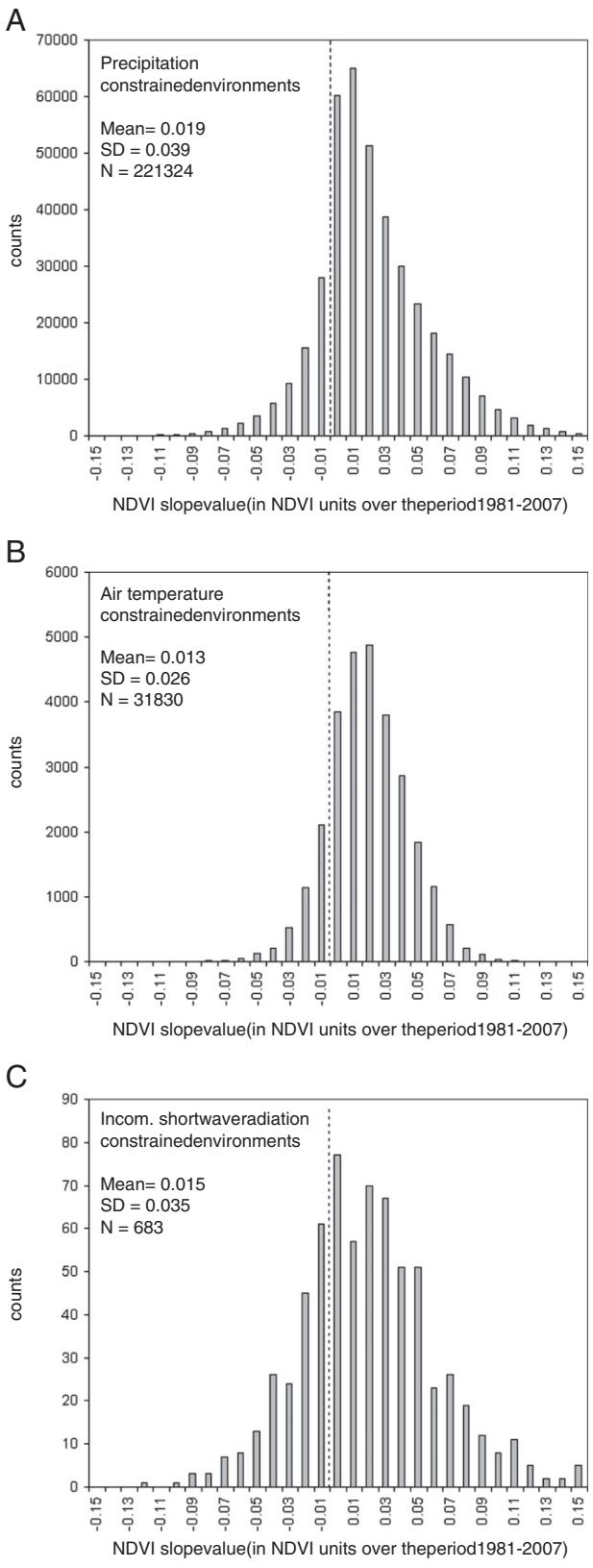

Fig. 5. Histograms of the NDVI slope in semi-arid areas from July 1981 to December 2007 in environments constrained by, (A) precipitation, (B) air temperature and (C) incoming shortwave radiation. Dashed veritcal line represents NDVI trend values of 0 (NDVI units over the total period 1981–2007). Note the different scale on the y-axis value for each sub-plot due to the different number of pixels in each category.

explained NDVI variance in semi-arid areas by precipitation and air temperature derived from multiple regression analysis is shown in Fig. 8C.

4.4. Intra-annual trends of NDVI and climatic drivers

The intra-annual variations of generalized monthly NDVI over the first and last six-year periods of the time series (1982–1987 and 2002–2007) are shown (Fig. 9A and C) for the 10 selected areas (Fig. 1C) (Section 3.4). Intra-annual changes for the 10 selected areas a priori constrained by precipitation (Fig. 9A) and by both precipitation and air temperature (Fig. 9c) (areas shown in Fig. 1C and coordinates are provided in Table 1) show widely different changes in annual variations to be discussed in Section 5.4.

5. Discussion

5.1. GIMMS NDVI quality assessment

The general level of high r-values for semi-arid areas across the globe gives confidence that the GIMMS NDVI trends calculated for the entire period studied (1981–2007) are reliable. This is in agreement with Fensholt and Rasmussen (2011) who showed that the correlation between GIMMS and MODIS NDVI is high for the 150–700 mm/year rainfall zone of the Sahel and Southern Africa. Globally, for the most sparsely vegetated areas in the arid zone lower correlations between GIMMS and MODIS NDVI were found by Fensholt and Proud (2012), not found between Terra and Aqua MODIS NDVI, thereby suggesting that trends in GIMMS data should be treated with caution for the arid areas. This agrees with the lower absolute r-values found in Fig. 2A for many semi-arid areas bordering the arid zone. Beck et al. (2011) studied the performance of four AVHRR-derived NDVI data sets (Pathfinder AVHRR Land (PAL); GIMMS; Land Long Term Data Record (LTDR) version 3 (V3); Fourier-Adjustment, Shortwave zenith angle corrected, Interpolated Reconstructed (FASIR)) using MODIS and Landsat imagery and concluded that temporal-change values of the GIMMS data set performed best amongst the four. Other studies have evaluated AVHRR based NDVI (including GIMMS) compatibility with newer sensors (the Système Pour l'Observation de la Terre (SPOT) VEGETATION, the Sea-viewing Wide Field-of-view Sensor (SeaWiFS), the MODIS and the Medium Resolution Imaging Spectrometer (MERIS)) (Brown et al., 2006; Pedelty et al., 2007; Swinnen and Veroustraete, 2008; Tucker et al., 2005).

5.2. Inter-annual trends in observed NDVI

The NDVI trends for semi-arid areas across the globe showing an overall greening (Fig. 3) contrast the results derived from ground based observations in dryland areas as synthesized in the Millennium Ecosystem Asessment (2005). Despite time-space specific differences in the performance of various AVHRR based NDVI datasets when intercompared (Slayback et al., 2003; Baldi et al., 2008; Fensholt et al., 2006; McCloy et al., 2005; Hall et al., 2006; Beck et al., 2011; de Jong et al., 2011) the NDVI trend results presented here correspond well with other studies based on different AVHRR datasets including semi-arid areas across the globe (Nemani et al., 2003; Young and Harris, 2005; Xiao and Moody, 2005; Beck et al., 2011; de Jong et al., 2011) or semi-arid areas on a continental/regional scale Globally: Hellden and Tottrup (2008); South America: Paruelo et al. (2004) and Baldi et al. (2008); Australia: Donohue et al. (2009); North America: Zhou et al. (2001) and Slayback et al. (2003); Sahel: Fensholt et al. (2009); Herrmann et al. (2005); Olsson et al. (2005); China: Li et al. (2010).

It is noteworthy that the LM test in general describes areas of positive global semi-arid NDVI trends better than the MK test, and the opposite is the case for areas characterized by negative NDVI trends. The difference in the explanatory power of the LM and MK tests for

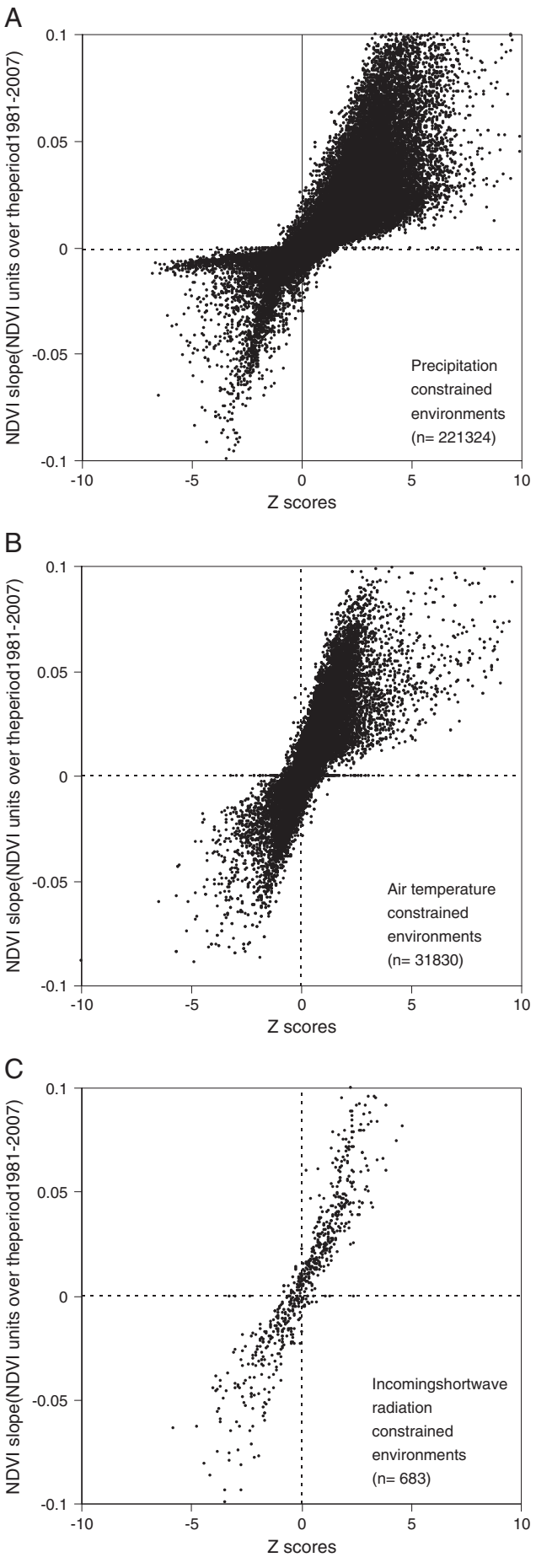

positive and negative NDVI trends (Fig. 4A and B) likely indicates different causal drivers for the observed NDVI changes (next section).

5.3. Inter-annual NDVI trend relationship with climatic drivers

Large regions of semi-arid areas with a significant decrease in precipitation (Fig. 7A) are located in USA and the border between eastern Mongolia/China and Russia whereas large regions of increased precipitation comprise southern Argentina, the Sahel, borders of Kazakhstan and China and areas in southern Africa and northern Australia. Trend analysis of air temperature reveals very limited areas of significantly decreased air temperatures in semi-arid areas across the globe and large areas characterized by significantly positive trends (Fig. 7B). The spatial distribution of these significant precipitation and air temperature trends matches in several case areas with significant changes in vegetation (Fig. 3). For areas like in Sahel, southern Africa, Venezuela and India (precipitation being the primary constraint to vegetation growth, Fig. 1C) there is a correspondence between increasing precipitation and greenness. Also for areas defined as being primarily air temperature constrained (Fig. 1C), like the northern central part of USA, central Turkey and Inner Mongolia, there is a correspondence between increasing vegetation trends and increasing air temperatures. Trends in air temperature for semi-arid areas are not straight forward to interpret since increased air temperatures might be favorable for vegetation growth in boreal regions whereas for warmer semi-arid areas increased air temperatures might reduce photosynthetic efficiency caused by decreasing leaf conductance and increased dark respiration (Hanan and Prince, 1997; Midgley et al., 2004). In many semi-arid regions of the world there has been a decrease in observed near-surface wind-speed (McVicar et al., 2012) which will result in lower evaporation rates thereby providing vegetation more opportunity to transpire moisture as opposed to moisture being lost via soil evaporation.

Not surprisingly, there is a good correspondence between vegetation dynamics and precipitation in most semi-arid areas (Fig. 8A) as also reflected in areas defined as being water constrained in Fig. 1C. There are also considerable areas in temperate zones characterized by insignificant ($p \geq 0.05$) relation between NDVI and precipitation and in the northernmost boreal regions the relation even becomes negative. For these zones the NDVI/air temperature correlation (Fig. 8B) increases as would be expected from Fig. 1C. However, there are also areas without positive correlations between trends in NDVI and trends of the variable defined as being the primary constraint to growth: in southern Argentina (constrained both by precipitation and air temperature) the negative vegetation trends (Fig. 3) but positive precipitation trends (Fig. 7A) and insignificant air temperature trends (Fig. 7B) generates an area with a significant negative correlation between NDVI and precipitation (Fig. 8A) and insignificant relation between NDVI and air temperature (Fig. 8B). The decreasing precipitation trend in the southern central USA (Fig. 7A) is also not reflected in uniform negative NDVI trends (Fig. 3) reflected in mixed areas of significantly positive, significantly negative and insignificant correlations between precipitation and NDVI (Fig. 8A).

The influence from anthropogenic disturbance from (changes in) agricultural practice including potential decoupling from climatic constraints by irrigation and use of fertilizers is important for the understanding of drivers of NDVI trends. By studying the spatio-temporal distribution of the relationship between vegetation dynamics and climate variables secondary indicators on the human impact on vegetation trends can potentially be inferred: if a poor relation exists between vegetation dynamics and the variable considered the a priori primary climatic constraint to growth this could indicate

Fig. 6. Scatterplots of significance (Z scores) of the NDVI slope in semi-arid areas from July 1981 to December 2007 versus the calculated NDVI slope value for areas constrained by (A) precipitation (B) air temperature and (C) incoming shortwave radiation.

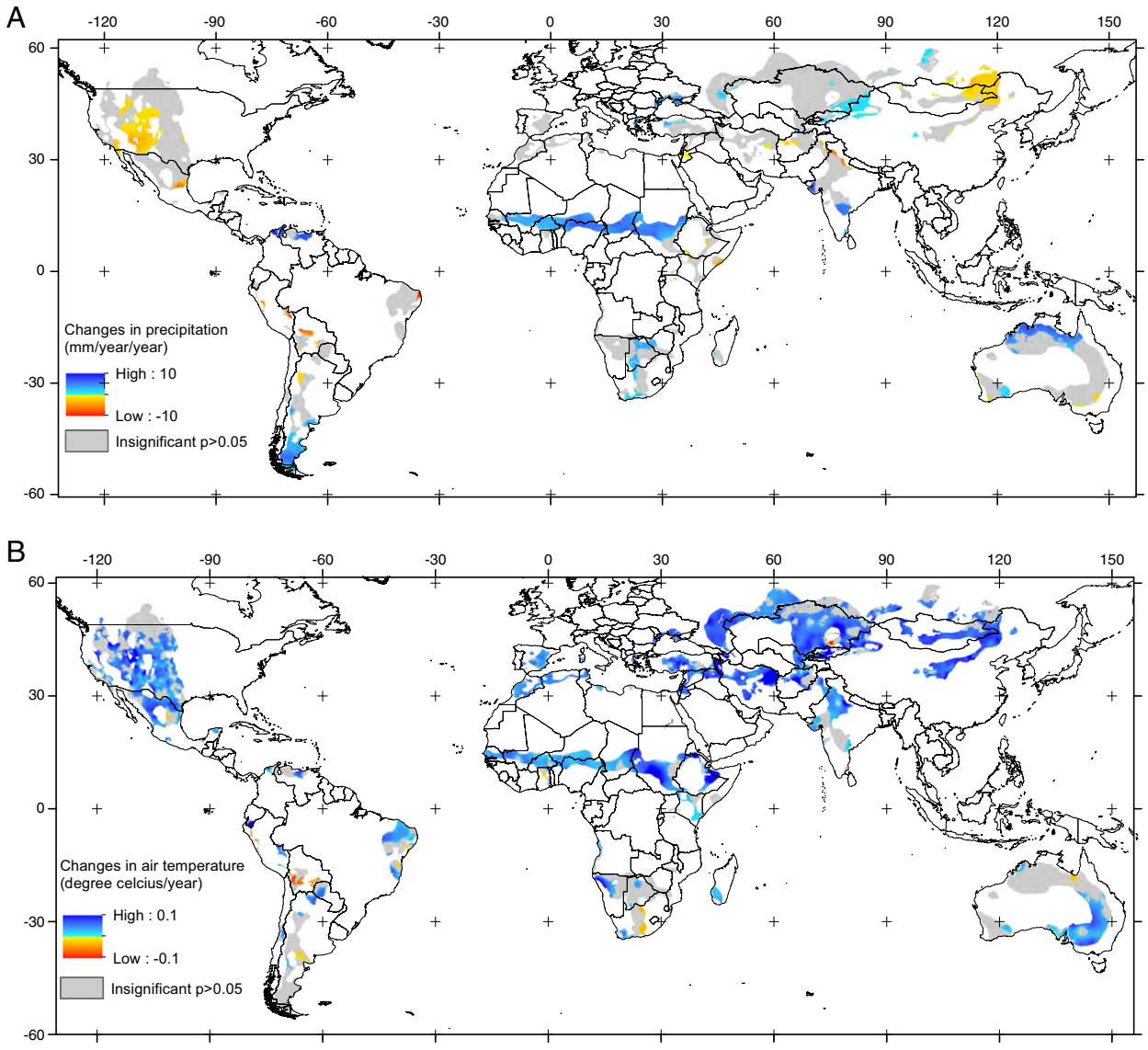

Fig. 7. Changes in (A) precipitation and (B) air temperature in semi-arid areas from July 1981 to December 2007. Only pixels with a statistically significant trend ($p<0.05$) are colored. (For interpretation of the references to color in this figure legend, the reader is referred to the web version of this article.)

perturbations from human activities. This approach however, is based on "evidence from absence" and can therefore never be more than indicative. The NDVI multiple regression with precipitation and air temperature (Fig. 8C) shows large spatial differences with highest explanatory power in northern Sahel, Southern Africa and northern Australia and mixed patterns from high to no explained variance for most temperate and boreal zones. Comparing areas of low explained NDVI variance and land cover classes in semi-arid areas characterized by anthropogenic influence (Fig. 1B, pink-purple colors) does not provide a clear correspondence. However, the presence of agriculture does not indicate the prevalence of irrigation and use of fertilizers and Sahelian agriculture (characterized by limited use of irrigation/fertilizers) is not expected to show a similar decoupling from climatic constraints as is the case for high-intensity industrial farming. Nevertheless, semi-arid areas of Spain, central Turkey, India and Southwestern Australia are all examples of regions dominated by agriculture with increasing NDVI trends not explained by climatic variables thereby suggesting human influence as a contributing cause.

The average global increase in NDVI (an increase of 0.015 NDVI units over the 1981–2007) regardless of the climatic driver conforms to the expectations, that the increase in atmospheric CO_2-concentration is likely to cause an increase in vegetation productivity. The CO_2 fertilization effect is supported by modeling studies (e.g., Bounoua et al., 2010), experimental studies (e.g., Ainsworth and Long, 2005; Polley et al., 2008), and previous remotely sensed based studies (e.g., Donohue et al., 2009). To determine the size of the CO_2 fertilization effect relative to trends in other climate variables however requires modeling. Satellite remote sensing is increasingly being used with ecosystem process models to provide new insights into the underlying causes of the trends observed in many of the world's dry environments (Hickler et al., 2005; Seaquist et al., 2009). Hickler et al. (2005) tested the extent to which climatic trends and atmospheric CO_2 concentration trends could account for the greening trend in the Sahel using LPJ-DGVM (Lund Potsdam Jena-Dynamic Global Vegetation Model Sitch et al., 2003). LPJ-DGVM was able to simulate the observed long-term greening trend (and its inter-annual variability) and an analysis of the model processes showed that precipitation was the primary cause of the modeled vegetation trend, with atmospheric CO_2 concentrations having only a minor positive effect. A recent study by Morgan et al. (2011) shows that annual grasses (c_4 type) in warmed semi-arid grasslands prosper from increased atmospheric CO_2 tending to eliminate the desiccation effect of moderate warming. The fact that productivity in semi-arid grasslands

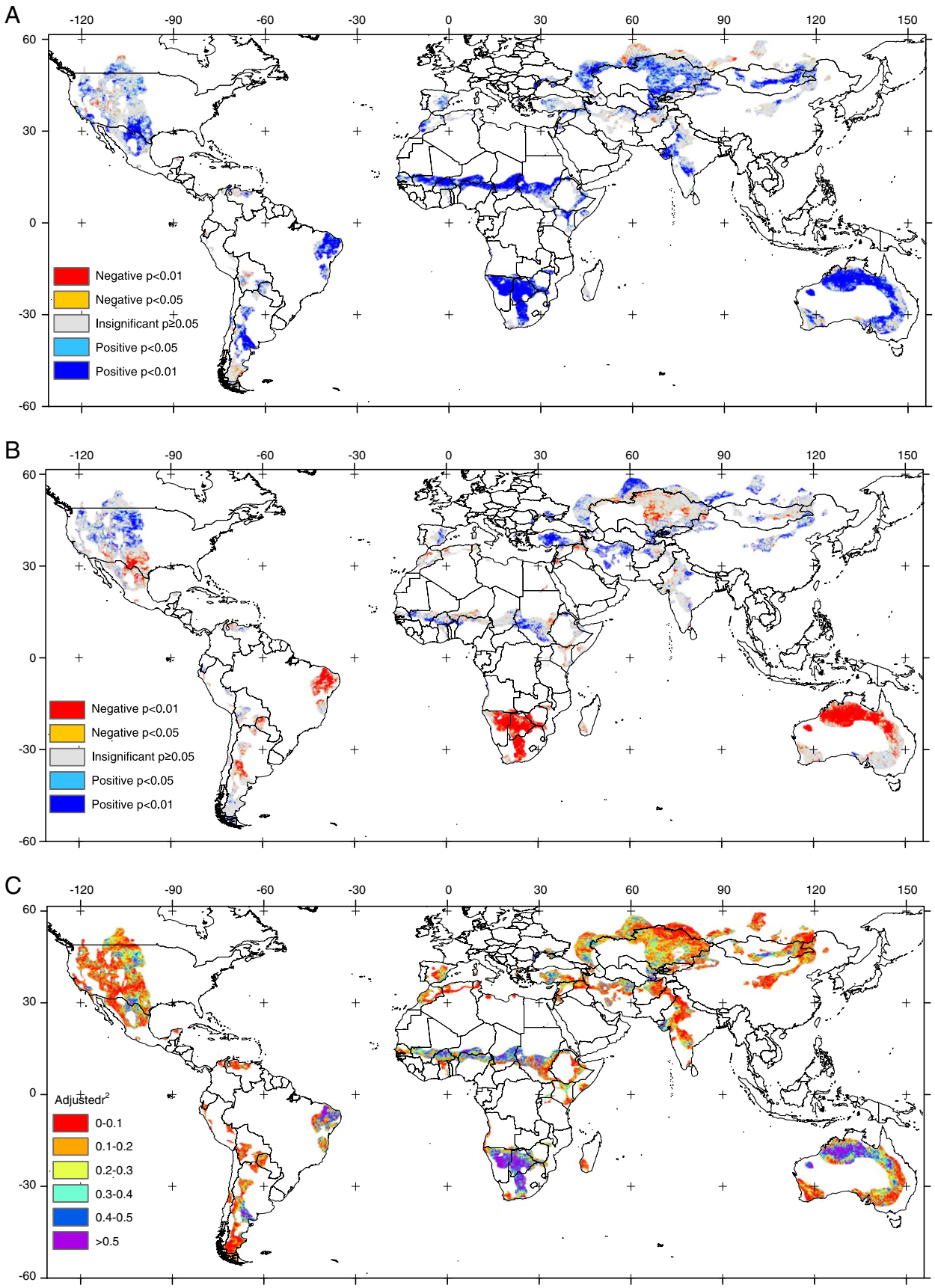

Fig. 8. (A) Significance of correlation between annual integrated GIMMS NDVI and annual summed GPCP precipitation 1982–2007. (B) Significance of correlation between annual integrated GIMMS NDVI and annual mean air temperature 1982–2007. (C) Multiple regression of annual summed GPCP precipitation and annual mean air temperature on annual integrated GIMMS NDVI 1982–2007(adjusted r2 values).

Table 3
Summary statistics of significant NDVI trends ($p<0.05$) (1981–2007) in semi-arid areas as a function of predominant potential climatic constraint variable.

			Significant NDVI trends		Significant NDVI trends coinciding with significant trends in climatic driver	
Predominant potential climatic constraint	Count (n)	Percentage (%)	Count (n)	Percentage (%)	Count (n)	Percentage (%)
Water availability	221,324	50.5	115,144	52.0	51,182	44.5
Air temperature	31,830	7.3	10,313	32.4	7703	74.7
Incoming shortwave radiation	683	0.2	40	19.8	Not calculated	

may gain more than expected in a warmer CO_2-enriched world supports the results presented here.

5.4. Intra-annual trends of NDVI and climatic drivers

Areas constrained by precipitation (Fig. 9A–B): in the Sahel the positive trend in NDVI (Fig. 3) appears to be related mainly to an increase in the maximum NDVI in the growing season, while the length of the growing season remains unchanged (de Jong et al., 2011; Heumann et al., 2007; Sobrino and Julien, 2011). The increasing annual precipitation trend of Sahel (Fig. 7A and B) primarily caused by higher precipitation values during summer months (Fig. 9B) suggests that the greening trend of Sahel is primarily precipitation driven; as also found by Hickler et al. (2005) and Huber et al. (2011). In India the increase in NDVI is uniform through the entire year (Fig. 9A) but only an increase in summer precipitation can be observed (Fig. 9B) (only part of the area was found to be characterized by significant positive trends in Fig. 7A). However, this change in precipitation seasonality cannot possibly explain the observed greening trend also found for winter months in India, pointing towards other drivers of change such as human influence. Particularly in view of India's higher population density than the Sahel this hypothesis is plausible (also supported by the land use map Fig. 1B) and Lee et al. (2009) found the greening of the Indian subcontinent (1982–2003) to be significantly correlated with increases in the irrigated area whereas no increase in precipitation was observed. In South-western Australia the NDVI increase is related to an increase during the Southern hemisphere autumn and winter, while NDVI-values in spring are unchanged (Fig. 9A). The increased precipitation in South-western Australia in April (Fig. 9B) could cause the NDVI increase during the Southern hemisphere fall and winter (May–August). However the precipitation trends decrease from May and onwards (the area is not characterized by significant precipitation trends, Fig. 7A) and also here anthropogenic influence from agriculture (Fig. 1B and Donohue et al., 2009) is likely to explain the significant greening trend. In the region covering Eastern Australia the NDVI decrease is caused by a winter and spring decrease (Fig. 9A). This corresponds to results by Donohue et al. (2009) who found both a positive trend in vegetation for South-western Australia and a negative trend in Eastern Australia to occur during Southern hemisphere winter. The Eastern Australia winter and spring decrease in NDVI is reflected in changes in precipitation seasonality with decreasing winter and spring values (Fig. 9B). Donohue et al. (2009) found the decrease in precipitation for Eastern Australia to be most pronounced during the spring using a gridded product based on a national network of meteorological stations. In northern Argentina the decrease in NDVI is observed throughout the year but most pronounced in the Southern hemisphere spring and summer growing season (October–February) (Fig. 9A). This agrees with the de Jong et al. (2011) findings who found a reduction in the length of growing season for this region. The decrease in NDVI during most months is reflected well in the change in precipitation (Fig. 9B) (as supported by Loyarte and Menenti, 2008), thereby likely to explain the greenness trends.

Areas constrained by precipitation and air temperature (Fig. 9C–E): for Turkey (Fig. 9C), the long-term increase in NDVI (Fig. 3) was the result of a substantial increase in the NDVI-level in spring and early summer (March–June). The noticeable NDVI increase in Turkey during spring is not reflected in strong changes in spring precipitation (Fig. 9D) or spring air temperature (Fig. 9E). Increased summer air temperatures are observed in 2002–2007, however succeeding the period during the year for which increased greenness was observed. The absence of explanatory capabilities of climatic drivers on both inter- and intra-annual scale suggests anthropogenic influence as supported by Fig. 1B. Central Turkey is also characterized by implementation of large scale river based irrigation schemes in the last part of the analysis period (Ozdogan et al., 2006). In Dakota, USA, the long-term increase in NDVI is reflected in a NDVI increase throughout the year, being most pronounced during June–July and in October–December (Fig. 9C). The observed greening in Dakota, USA does not reflect any trends of the climatic constraints (Fig. 9D–E). The land use classification does not indicate intensive human influence in this area primarily covered by the class “Herbaceous Cover, closed–open”, however the greening of Dakota has been suggested to be partly related to changes in irrigation practices (Neigh et al., 2008). The SW Russia long-term NDVI increase is related to greener conditions during early spring to summer, dominating over the observed decrease in the fall (Fig. 9C). The increased spring greenness coincides with a moderate increase in precipitation (Fig. 9D). More important for the greening is probably the noticeable increase in air temperature from February and throughout the spring which has advanced above 0 °C by approximately one month (Fig. 9E) as also discussed in Delbart et al. (2008). The Central Kazakhstan long-term decrease in NDVI (Fig. 3) as also reported by de Jong et al. (2011) is caused by decreasing summer NDVI values (Fig. 9C). The declining greenness during summer months corresponds with the driest period of the year. No changes in the limited precipitation are observed over the period (Fig. 9D) but the air temperature has increased noticeably during spring and early summer months which potentially could cause a larger water deficit from evapotranspiration losses. de Beurs and Henebry (2004) found a general increase in NDVI for most regions of Kazakhstan using the AVHRR Land (PAL) data from 1982 to 1999 attributed extensive land cover/land use change from the institutional changes surrounding the disintegration of the Soviet Union in the early 1990s. However a more recent paper by same authors (de Beurs et al., 2009) based on MODIS data 2000–2008 reports a significant decrease in NDVI for Kazakhstan caused be several years of summer drought. In southern Argentina, the decreasing NDVI trend is reflected in a general NDVI decrease throughout the year. The areas are characterized by relatively sparse vegetation (lowest NDVI values in Fig. 9C) and is primarily covered by “Sparse herbaceous or sparse shrub cover” (Fig. 1B). The decreasing NDVI trends apparent over the full year cannot be explained by air temperatures being constant over the time period studied (Fig. 9E). Precipitation has significantly increased during the period (Fig. 7B) and the intra-annual analysis reveals a change towards higher precipitation amounts during all months (Fig. 9D). The possibility that the GIMMS dataset might not capture correctly the greenness trend in this area cannot be excluded (as discussed in Baldi et al., 2008). The NDVI seasonality is low causing a decreased signal-to-noise ratio and this area also shows low correspondence between

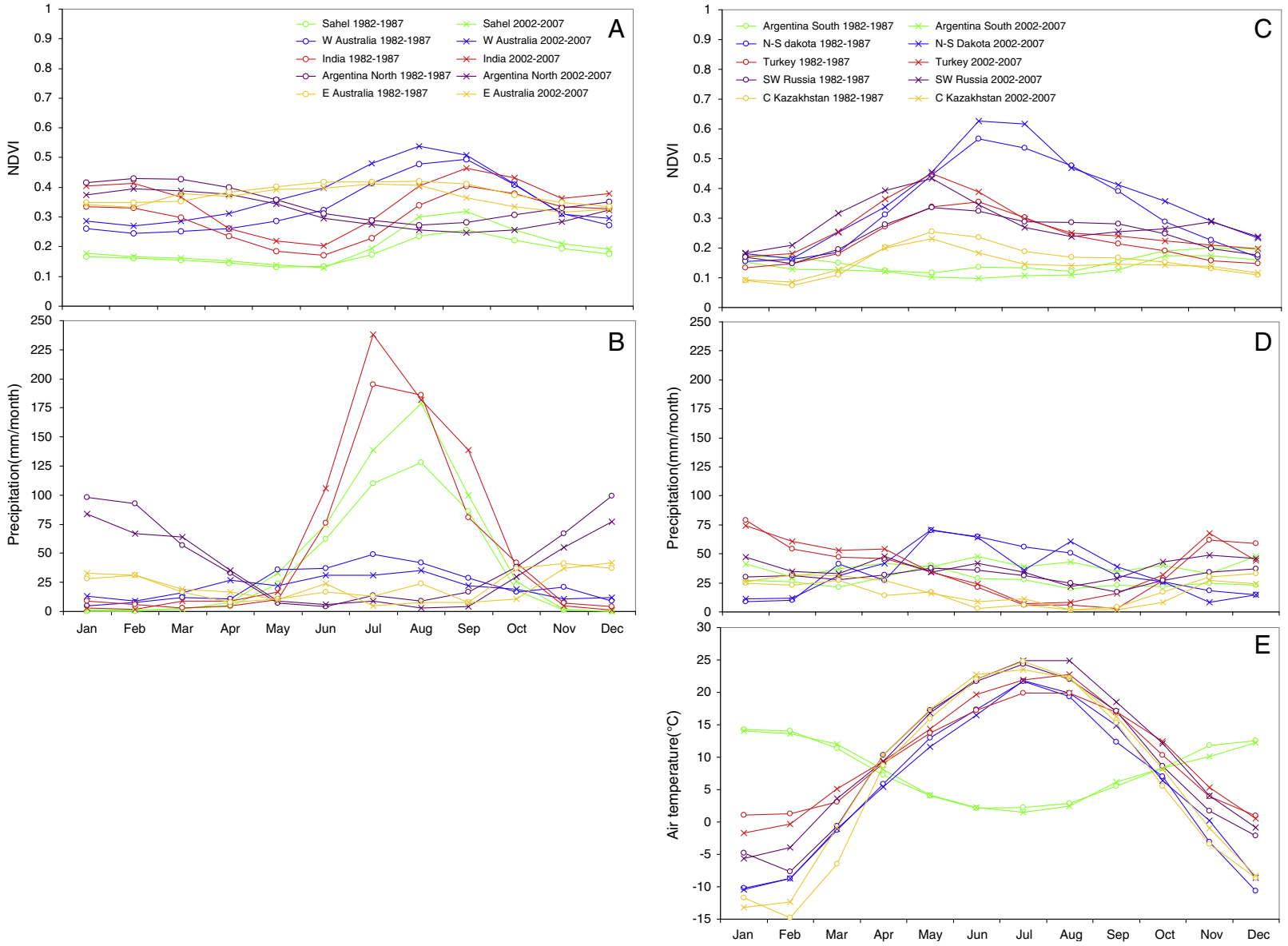

Fig. 9. Intra-annual variation of monthly NDVI and climatic constraints for each of the selected areas (Table 1 and Fig. 1c): (A) NDVI seasonal curves for precipitation constrained areas. (B) Precipitation seasonal curves for precipitation constrained areas. (C) NDVI seasonal curves for precipitation/temperature constrained areas. (D) Precipitation seasonal curves for precipitation/temperature constrained areas. (E) Air temperature seasonal curves for precipitation/temperature constrained areas. Curves represent 1982–1987 and 2002–2007 harmonic regression fitted values.

GIMMS and MODIS NDVI in Fig. 2A. The reason for the decreasing NDVI trends in this sparsely populated area remains a question for further research.

6. Conclusion

Semi-arid areas are assumed to be particularly vulnerable to climate variability and change, and given the growing political attention to climate adaptation and community resilience to climate change, there are strong reasons to inform national and international policies in the best possible way. As biological production is important to livelihood systems in most semi-arid areas, improved understanding of their functioning (monitoring, modeling and projection of changes in vegetation greenness and productivity) provide crucial knowledge in preparing for the adaptation measures required.

The 27-year time series of satellite data analyzed here provides a unique assessment of the spatial and temporal changes in NDVI for semi-arid areas of the world. Inter-annual trends and changes can be described in great detail and intra-annual variations can provide a more detailed indication of differences in the nature of inter-annual trends. While inter-annual trends in NDVI can only give indications of causal relationships when combined with information on potential climatic growth constraints, analysis of changes in intra-annual variation of NDVI does allow certain causes to be inferred, or at least may provide the catalyst for causal hypothesis generation, which could be tested where other data-sources are available. The results presented clearly show that there is no basis for suggesting that semi-arid areas across the globe have similar trends in vegetation greenness. While the global average trend is positive, the local and regional trends reveal considerable variation in direction and magnitude of change. Testing for regional scale causes of NDVI trends was conducted from combined time series analysis of precipitation and air temperature. Results show that many regional-scale greening patterns in semi-arid areas are sufficiently coherent and consistent with correlated variables to form the basis of national and international policy.

Acknowledgment

The current paper was initiated by the Global Land Project, a joint project under the International Geosphere Biosphere Program (IGBP) and the International Human Dimension Program (IHDP). The authors are grateful to the Global Land Project, International Project Office (GLP-IPO) for preparing, funding and facilitating the workshop held in Copenhagen. The authors would like to thank R. Nemani for providing the potential climatic plant growth constraints data used in the analyses. Finally the authors are grateful to the anonymous reviewers for their many detailed and constructive comments that considerably improved the manuscript.

References

Adler, R. F., Huffman, G. J., Chang, A., Ferraro, R., Xie, P. P., Janowiak, J., et al. (2003). The version-2 global precipitation climatology project (GPCP) monthly precipitation analysis (1979-present). *Journal of Hydrometeorology*, *4*, 1147–1167.

Ainsworth, E. A., & Long, S. P. (2005). What have we learned from 15 years of free-air CO(2) enrichment (FACE)? A meta-analytic review of the responses of photosynthesis, canopy. *New Phytologist*, *165*, 351–371.

Anyamba, A., & Tucker, C. J. (2005). Analysis of Sahelian vegetation dynamics using NOAA-AVHRR NDVI data from 1981–2003. *Journal of Arid Environments*, *63*, 596–614.

Bai, Z. G., Dent, D. L., Olsson, L., & Schaepman, M. E. (2008). Proxy global assessment of land degradation. *Soil Use and Management*, *24*, 223–234.

Baldi, G., Nosetto, M. D., Aragon, R., Aversa, F., Paruelo, J. M., & Jobbagy, E. G. (2008). Long-term satellite NDVI data sets: Evaluating their ability to detect ecosystem functional changes in south America. *Sensors-Basel*, *8*, 5397–5425.

Bartholomé, E., Belward, A. S., Achard, F., Bartalev, S., Carmona-Moreno, C., Eva, H., et al. (2002). *GLC 2000: Global Land Cover mapping for the year 2000, EUR 20524 EN, European Commission, Luxembourg.* http://eccad.sedoo.fr/eccad_extract_interface/doc/pdf/GLC2000.pdf

Beck, H. E., McVicar, T. R., van Dijk, A. I. J. M., Schellekens, J., de Jeu, R. A. M., & Bruijnzeel, L. A. (2011). Global evaluation of four AVHRR-NDVI data sets: Intercomparison and assessment against Landsat imagery. *Remote Sensing of Environment*, *115*, 2547–2563.

Bounoua, L., Hall, F. G., Sellers, P. J., Kumar, A., Collatz, G. J., Tucker, C. J., et al. (2010). Quantifying the negative feedback of vegetation to greenhouse warming: A modeling approach. *Geophysical Research Letters*, *37*.

Brown, M. E., Pinzon, J. E., Didan, K., Morisette, J. T., & Tucker, C. J. (2006). Evaluation of the consistency of long-term NDVI time series derived from AVHRR, SPOT-Vegetation, SeaWiFS, MODIS, and Landsat ETM + sensors. *IEEE Transactions on Geoscience and Remote Sensing*, *44*, 1787–1793.

de Beurs, K. M., & Henebry, G. M. (2004). Land surface phenology, climatic variation, and institutional change: Analyzing agricultural land cover change in Kazakhstan. *Remote Sensing of Environment*, *89*, 497–509.

de Beurs, K. M., Wright, C. K., & Henebry, G. M. (2009). Dual scale trend analysis for evaluating climatic and anthropogenic effects on the vegetated land surface in Russia and Kazakhstan. *Environmental Research Letters*, *4*.

de Jong, R., de Bruin, S., de Wit, A., Schaepman, M. E., & Dent, D. L. (2011). Analysis of monotonic greening and browning trends from global NDVI time-series. *Remote Sensing of Environment*, *115*, 692–702.

Delbart, N., Picard, G., Le Toans, T., Kergoat, L., Quegan, S., Woodward, I., et al. (2008). Spring phenology in boreal Eurasia over a nearly century time scale. *Global Change Biology*, *14*, 603–614.

Donohue, R. J., McVicar, T. R., & Roderick, M. L. (2009). Climate-related trends in Australian vegetation cover as inferred from satellite observations, 1981–2006. *Global Change Biology*, *15*, 1025–1039.

Eastman, J. R., Sangermano, F., Ghimire, B., Zhu, H. L., Chen, H., Neeti, N., et al. (2009). Seasonal trend analysis of image time series. *International Journal of Remote Sensing*, *30*, 2721–2726.

Fan, Y., & van den Dool, H. (2008). A global monthly land surface air temperature analysis for 1948-present. *Journal of Geophysical Research-Atmospheres*, *113*.

Fensholt, R., Nielsen, T. T., & Stisen, S. (2006). Evaluation of AVHRR PAL and GIMMS 10-day composite NDVI time series products using SPOT-4 vegetation data for the African continent. *International Journal of Remote Sensing*, *27*, 2719–2733.

Fensholt, R., & Proud, S. R. (2012). Evaluation of Earth Observation based global long term vegetation trends - Comparing GIMMS and MODIS global NDVI time series. *Remote Sensing of Environment*, *119*, 131–147.

Fensholt, R., & Rasmussen, K. (2011). Analysis of trends in the Sahelian 'rain-use efficiency' using GIMMS NDVI, RFE and GPCP rainfall data. *Remote Sensing of Environment*, *115*, 438–451.

Fensholt, R., Rasmussen, K., Nielsen, T. T., & Mbow, C. (2009). Evaluation of earth observation based long term vegetation trends — Intercomparing NDVI time series trend analysis consistency of Sahel from AVHRR GIMMS, Terra MODIS and SPOT VGT data. *Remote Sensing of Environment*, *113*, 1886–1898.

Hall, F., Masek, J. G., & Collatz, G. J. (2006). Evaluation of ISLSCP Initiative IIFASIR and GIMMS NDVI products and implications for carbon cycle science. *Journal of Geophysical Research-Atmospheres*, *111*.

Hanan, N. P., & Prince, S. D. (1997). Stomatal conductance of west-central supersite vegetation in HAPEX-Sahel: Measurements and empirical models. *Journal of Hydrology*, *189*, 536–562.

Hellden, U., & Tottrup, C. (2008). Regional desertification: A global synthesis. *Global and Planetary Change*, *64*, 169–176.

Herrmann, S. M., Anyamba, A., & Tucker, C. J. (2005). Recent trends in vegetation dynamics in the African Sahel and their relationship to climate. *Global Environmental Change*, *15*, 394–404.

Heumann, B. W., Seaquist, J. W., Eklundh, L., & Jonsson, P. (2007). AVHRR derived phenological change in the Sahel and Soudan, Africa, 1982–2005. *Remote Sensing of Environment*, *108*, 385–392.

Hickler, T., Eklundh, L., Seaquist, J. W., Smith, B., Ardo, J., Olsson, L., et al. (2005). Precipitation controls Sahel greening trend. *Geophysical Research Letters*, *32*.

Hill, J., Stellmes, M., Udelhoven, T., Roder, A., & Sommer, S. (2008). Mediterranean desertification and land degradation Mapping related land use change syndromes based on satellite observations. *Global and Planetary Change*, *64*, 146–157.

Hoaglin, D. C., Mosteller, F., & Tukey, J. W. (2000). *Understanding robust and exploratory data analysis.* New York: Wiley.

Huber, S., Fensholt, R., & Rasmussen, K. (2011). Water availability as the driver of vegetation dynamics in the African Sahel from 1982 to 2007. *Global and Planetary Change*, *76*, 186–195.

Huete, A., Didan, K., Miura, T., Rodriguez, E. P., Gao, X., & Ferreira, L. G. (2002). Overview of the radiometric and biophysical performance of the MODIS vegetation indices. *Remote Sensing of Environment*, *83*, 195–213.

Huete, A. R., Jackson, R. D., & Post, D. F. (1985). Spectral response of a plant canopy with different soil backgrounds. *Remote Sensing of Environment*, *17*, 37–53.

Kanamitsu, M., Ebisuzaki, W., Woollen, J., Yang, S. K., Hnilo, J. J., Fiorino, M., et al. (2002). Ncep-Doe Amip-Ii reanalysis (R-2). *Bulletin of the American Meteorological Society*, *83*, 1631–1643.

Kendall, M. (1938). A new measure of rank correlation. *Biometrika*, *30*(1–2), 81–89.

Lee, E., Chase, T. N., Rajagopalan, B., Barry, R. G., Biggs, T. W., & Lawrence, P. J. (2009). Effects of irrigation and vegetation activity on early Indian summer monsoon variability. *International Journal of Climatology*, *29*, 573–581.

Li, B., Wang, J., & Yu, W. (2010). Recent trends in vegetation greenness and their causes in semiarid areas of China. *Multimedia Technology (ICMT)*, 1–7.

Loyarte, M. M. G., & Menenti, M. (2008). Impact of rainfall anomalies on Fourier parameters of NDVI time series of northwestern Argentina. *International Journal of Remote Sensing*, *29*, 1125–1152.

McCloy, K. R., Los, S., Lucht, W., & Højsgaard, S. (2005). A comparative analysis of three long-term NDVI datasets derived from AVHRR satellite data. *EARSeL eProceedings*, *4* (1), 52–69.

McVicar, T. R., Roderick, M. L., Donohue, R. J., Li, L. T., Van Niel, T. G., Thomas, A., et al. (2012). Global review and synthesis of trends in observed terrestrial near-surface wind speeds: Implications for evaporation. *Journal of Hydrology*, *416–417*, 182–205.

Midgley, G. F., Aranibar, J. N., Mantlana, K. B., & Macko, S. (2004). Photosynthetic and gas exchange characteristics of dominant woody plants on a moisture gradient in an African savanna. *Global Change Biology*, *10*, 309–317.

Millennium Ecosystem Asessment (2005). *Ecosystems and human wellbeing: Desertification synthesis.* Washington DC: World Resources Institute http://www.maweb.org/documents/document.355.aspx.pdf

Morgan, J. A., LeCain, D. R., Pendall, E., Blumenthal, D. M., Kimball, B. A., Carrillo, Y., et al. (2011). C(4) grasses prosper as carbon dioxide eliminates desiccation in warmed semi-arid grassland. *Nature*, *476*, 202–205.

Neigh, C. S. R., Tucker, C. J., & Townshend, J. R. G. (2008). North American vegetation dynamics observed with multi-resolution satellite data. *Remote Sensing of Environment*, *112*, 1749–1772.

Nemani, R. R., Keeling, C. D., Hashimoto, H., Jolly, W. M., Piper, S. C., Tucker, C. J., et al. (2003). Climate-driven increases in global terrestrial net primary production from 1982 to 1999. *Science*, *300*, 1560–1563.

Olsson, L., Eklundh, L., & Ardo, J. (2005). A recent greening of the Sahel — Trends, patterns and potential causes. *Journal of Arid Environments*, *63*, 556–566.

Ozdogan, M., Woodcock, C. E., Salvucci, G. D., & Demir, H. (2006). Changes in summer irrigated crop area and water use in Southeastern Turkey from 1993 to 2002: Implications for current and future water resources. *Water Resources Management*, *20*, 467–488.

Paruelo, J. M., Garbulsky, M. F., Guerschman, J. P., & Jobbagy, E. G. (2004). Two decades of Normalized Difference Vegetation Index changes in South America: Identifying the imprint of global change. *International Journal of Remote Sensing*, *25*, 2793–2806.

Pedelty, J., Devadiga, S., Masuoka, E. B., Pinzon, J. M., Tucker, C. J., Vermote, E. F., et al. (2007). Generating a long-term land data record from the AVHRR and MODIS Instruments. Geoscience and Remote Sensing Symposium, 2007. IGARSS 2007. *IEEE International*, 1021–1025.

Polley, H. W., Johnson, H. B., Fay, P. A., & Sanabria, J. (2008). Initial response of evapotranspiration from tallgrass prairie vegetation to CO2 at subambient to elevated concentrations. *Functional Ecology*, *22*, 163–171.

Prince, S. D., Wessels, K. J., Tucker, C. J., & Nicholson, S. E. (2007). Desertification in the Sahel: A reinterpretation of a reinterpretation. *Global Change Biology*, *13*, 1308–1313.

Seaquist, J. W., Hickler, T., Eklundh, L., Ardo, J., & Heumann, B. W. (2009). Disentangling the effects of climate and people on Sahel vegetation dynamics. *Biogeosciences*, *6*, 469–477.

Sen, P. K. (1968). Estimates of the regression coefficient based on Kendall's tau. *Journal of the American Statistical Association*, *63*, 1379–1389.

Sitch, S., Smith, B., Prentice, I. C., Arneth, A., Bondeau, A., Cramer, W., et al. (2003). Evaluation of ecosystem dynamics, plant geography and terrestrial carbon cycling in the LPJ dynamic global vegetation model. *Global Change Biology*, *9*, 161–185.

Slayback, D. A., Pinzon, J. E., Los, S. O., & Tucker, C. J. (2003). Northern hemisphere photosynthetic trends 1982–99. *Global Change Biology*, *9*, 1–15.

Sobrino, J. A., & Julien, Y. (2011). Global trends in NDVI-derived parameters obtained from GIMMS data. *International Journal of Remote Sensing*, *32*, 4267–4279.

Solano, R., Didan, K., Jacobson, A., & Huete, A. (2010). MODIS vegetation indices (MOD13) C5 user's guide. (Available at:) http://tbrs.arizona.edu/project/MODIS/UsersGuide.pdf

Swinnen, E., & Veroustraete, F. (2008). Extending the SPOT-VEGETATION NDVI time series (1998–2006) back in time with NOAA-AVHRR data (1985–1998) for southern Africa. *IEEE Transactions on Geoscience and Remote Sensing*, *46*, 558–572.

Theil, H. (1950). A rank-invariant method of linear and polynomial regression analysis. I, II and III. *Proceedings of Koninklijke Nederlandse Akademie van Wetenschappen*, *53*. (pp. 386–392) (521–525, 1397–1412).

Tucker, C. J., Pinzon, J. E., Brown, M. E., Slayback, D. A., Pak, E. W., Mahoney, R., et al. (2005). An extended AVHRR 8-km NDVI dataset compatible with MODIS and SPOT vegetation NDVI data. *International Journal of Remote Sensing*, *26*, 4485–4498.

United Nations Environment Programme, Middleton, N., & Thomas, D. S. G. (1997). World atlas of desertification. *London; New York New York: Arnold; Copublished in the US, Central and South America by John Wiley*.

Vermote, E. F., El Saleous, N. Z., & Justice, C. O. (2002). Atmospheric correction of MODIS data in the visible to middle infrared: First results. *Remote Sensing of Environment*, *83*, 97–111.

Wang, X. L. L., & Swail, V. R. (2001). Changes of extreme wave heights in Northern Hemisphere oceans and related atmospheric circulation regimes. *Journal of Climate*, *14*, 2204–2221.

Xiao, J., & Moody, A. (2005). Geographical distribution of global greening trends and their climatic correlates: 1982–1998. *International Journal of Remote Sensing*, *26*, 2371–2390.

Young, S. S., & Harris, R. (2005). Changing patterns of global-scale vegetation photosynthesis, 1982–1999. *International Journal of Remote Sensing*, *26*, 4537–4563.

Zhou, L. M., Tucker, C. J., Kaufmann, R. K., Slayback, D., Shabanov, N. V., & Myneni, R. B. (2001). Variations in northern vegetation activity inferred from satellite data of vegetation index during 1981 to 1999. *Journal of Geophysical Research-Atmospheres*, *106*, 20069–20083.